Supporting Information for

Mechanisms Underlying the Mpemba Effect in Water from Molecular Dynamics Simulation

Jaehyeok Jin [a†], William A. Goddard III [bc*]

[a] Department of Chemistry, Korea Advanced Institute of Science & Technology (KAIST), Daejeon 305-701, Korea

[b] Graduate School of EEWS, Korea Advanced Institute of Science and Technology, Daejeon 305-701, Korea

[c] Materials and Process Simulation Center, California Institute of Technology, 1200 East California Boulevard, Pasadena, California 91125, United States

[†] Present address: Department of Chemistry, University of Chicago, 5735 South Ellis Avenue, Chicago, Illinois 60637, United States

[*] to whom correspondence should be sent. E-mail: wag@wag.caltech.edu

A. Supporting information for well-described behavior of the supercooled water

(a) Similarity of the supercooled water with experiments and previous calculations

We calculated the AUC (area under curve) to compare the similarity of the supercooled DOS by experiments (INS), WHBB potential and our 2PT method. Areas were simply calculated by using a trapezoid method in the frequency domain, which is restricted up to 1000 cm^{-1}.

Table S1: Similarity of quenched changes in supercooled water

Method	Area under curve (cm^{-1})
WHBB potential[1]	327.0735 (cm^{-1})
INS experimental[2]	351.5980 (cm^{-1})
Present work	311.9084 (cm^{-1})

(b) Temperature dependence of supercooled water

It is well known that the supercooled water transforms to the ice structure below about 225K.[3] Thus, we considered rapid quenching from 370K to various final temperatures to this tendency. The default case (100K) was carried out by quenching it from 370K water to 100K over 50 ps. For same 50 ps period, we obtained supercooled states by quenched from 370K to 150, 200, 250, and 300K. The results are shown in Figure Sl-(a). The very low-frequency region, from 0 to 10 cm^{-1} (which mostly corresponds to diffusion) shows that the supercooled state is obtained for the quenches to 100K and perhaps for the quenches to 150K and maybe 200K. However the result of quenching to 250K and 300K are clearly not supercooled (far too much diffusion). Comparing the final quenches over the region up to 80 cm^{-1} we see that the modes from 0 to 50 cm^{-1} are shifted to 50-80 cm^{-1} as the final temperature is decreased. Interesting here is region II (80 to 155 cm^{-1}). We see that the quenches to the higher temperature have lower DOS for 80-88 cm^{-1}, higher for 88-100 cm^{-1} and lower for 100-155 cm^{-1}. This might indicate that 80-88 cm^{-1} and 100-155 cm^{-1} might be important for rapidly forming ice, but not the region from 88 to 100 cm^{-1}.

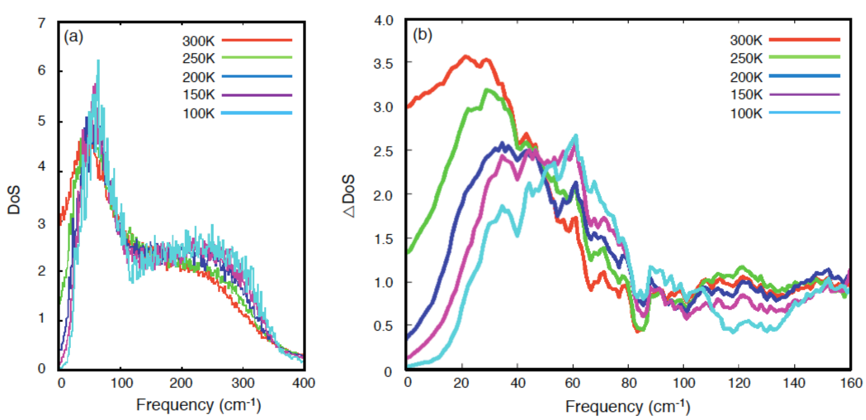

Figure S1. Examination of the DOS for water rapidly quenched from 370K to various temperatures (a) Final translational libration DOS of supercooled waters with different final temperatures (b) Differences of DOS between supercooled waters and pure ice Ih

B. Supplementary figures for the translational librational DOS spectrum with various quench times

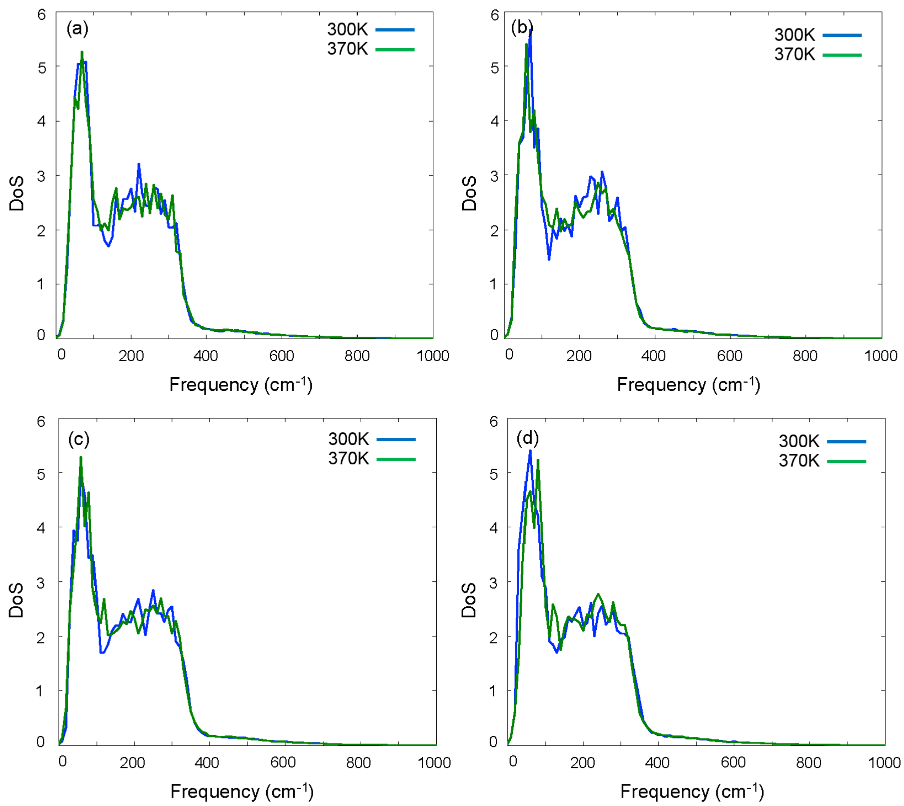

Figure S2: Translational librational DOS of the supercooled water with different total quench times (a) 20 ns (b) 4 ns (c) 2 ns (d) 0.5 ns

C. Extension of the time-scale while quenching

In Figure 2, the time evolution of the DOS was simulated by 50 ps and 500,000 ps. To guarantee the simulation to understand the Mpemba effect as macroscopic experiment, we extended the total quench time from 50 ps to 500, 5,000 and 50,000 and 500,000 ps in the same quenching process and analyzed the similarity of the evolution pattern.

(a) 500ps

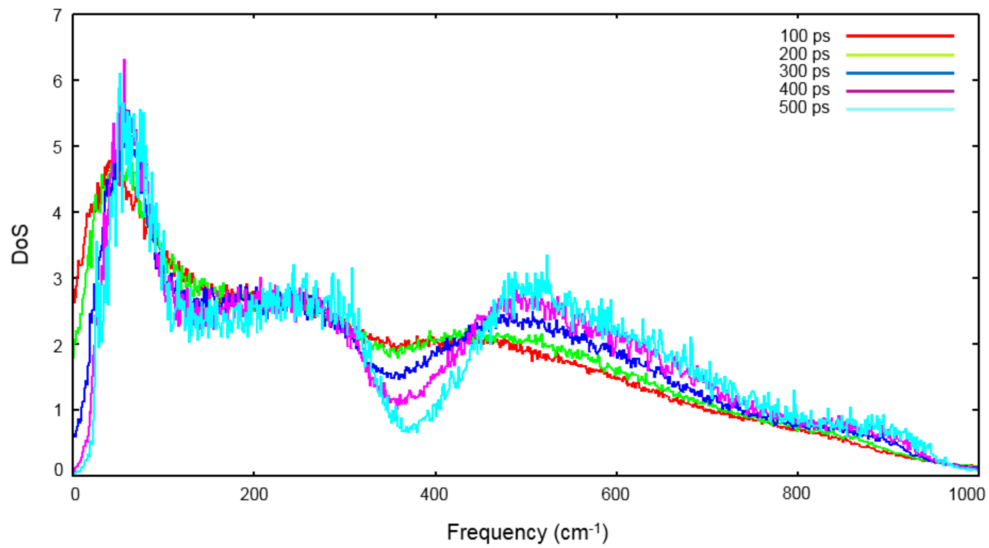

Figure S3: Changes in the Total DOS while quenching from 370K to 100K over 500ps

(b) 5,000ps

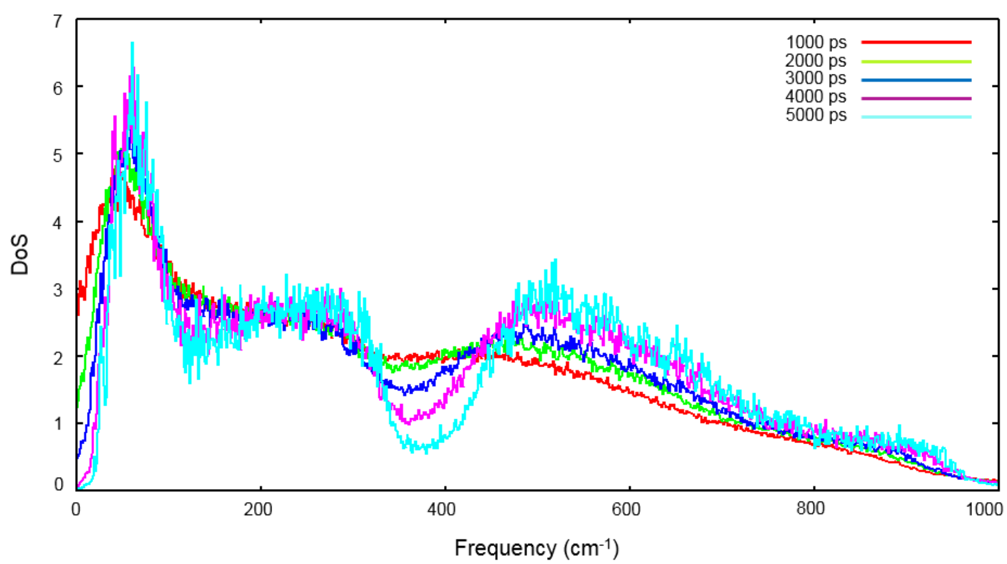

Figure S4: Changes in the Total DOS while quenching from 370K to 100K over 5,000ps

(c) 50,000ps

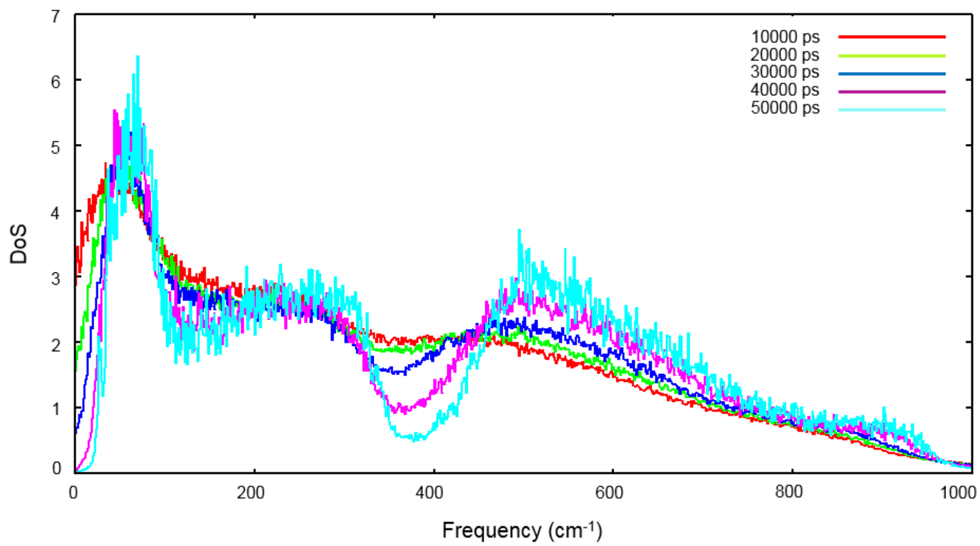

Figure S5: Changes in the Total DOS while quenching from 370K to 100K over 50,000ps

(d) 500,000ps

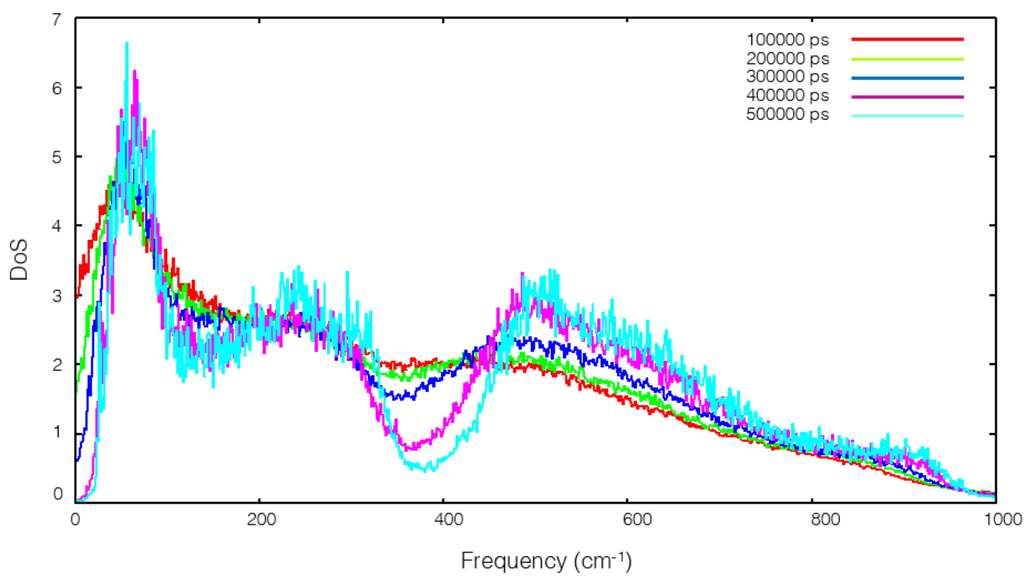

Figure S6: Changes in the Total DOS while quenching from 370K to 100K over 500,000ps

D. Dependency of the initial temperature in the supercooled water

In Table 2, we discussed about the correlation coefficient of water the supercooled from various initial temperatures. Also, we depicted the translational librational DOS of the supercooled water with three distinct temperatures: 300, 335, 370K to visualize the dependency of the initial temperature, see Figure S7. As stated previously, the supercooled water from 370K shows the minimum DOS in regime II, while the supercooled water from 370K represents the maximum DOS in regime II. The supercooled water from 335K shows the intermediate state between these two states. Also, in regime II, we also depicted the DOS of pure ice Ih and it resembles to the supercooled water from 370K.

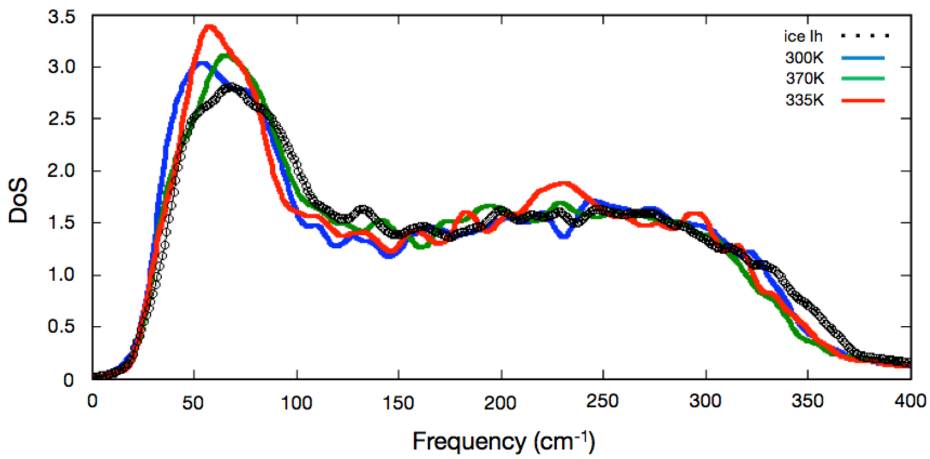

Fig S7: Translational librational DOS from the supercooled waters from various temperatures and pure ice Ih at 100K

E. Supplementary figures for modified mass simulation

In Figure 4, we figured out three major peaks induced by hexagonal motions of water in the modified mass simulation. Figure S8 shows the difference of DOS between modified cases and pure ice Ih.

After scaling by SQRT(4/18), the range of Figure S8-(a) corresponds to the regime I and the range of Figure S8-(b) corresponds to the regime III, especially up to 377 cm^{-1}. Firstly, the entangled behavior of DOS in Figure S8-(a) is distinguished as two main parts: 0-80 cm^{-1} and 80-170 cm^{-1}. First part shows fluctuating behavior. It can be interpreted by the mixed motions of acoustic translations of H_2O, which are observed at the frequency lower than 50 cm^{-1} (~ 106 cm^{-1} in modified case). After 106 cm^{-1}, the only peak observed is located in the range of 100 to 110 cm^{-1} and this peak is known as the specific translation mode induced by hexagonal acoustic translational mode.[3, 4] However, after 340 cm^{-1}, overall DOS shows no distinct peak in the depicted region.

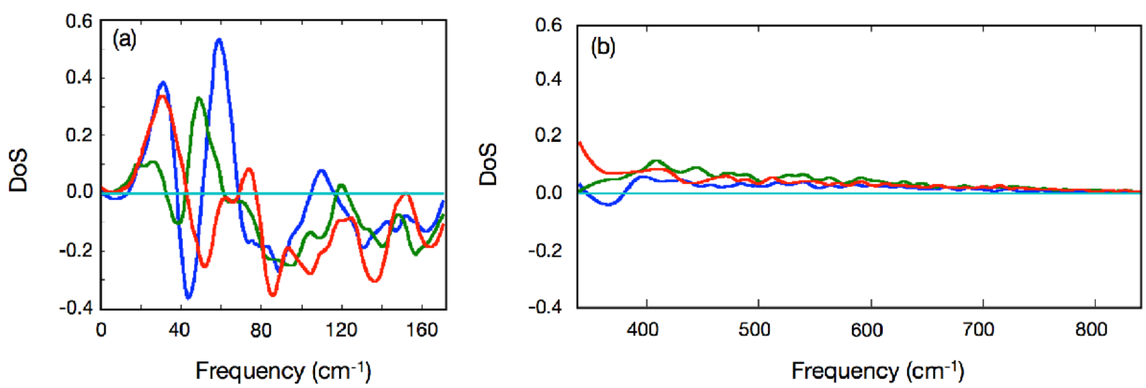

Figure S8: Difference between translational librational DOS of supercooled water at 100K with either the masses of a hexagon or a fused decamer or distinct hexagons modified and pure ice Ih: (a) 0-170 cm^{-1} (b) 170-340 cm^{-1}

F. Evolution of the DOS for supercooled water

To further examine the character of supercooled water quenched from various initial temperatures, we took the two cases of quenching from 370K and 300K to 100K, heated back to 250K for 750 ps and then requenched the system to 100K over 750 ps. For each 150 ps, we compared the two cases and found that the evolution to form supercooled water from the 370K case leads to a more ice-like DOS than the one for which from the 300K case. This indicates that the supercooled water quenched from 370K to 100K evolves toward ice faster after annealing at 250K and requenching to 100K, than for the case of quenching from 300K case.

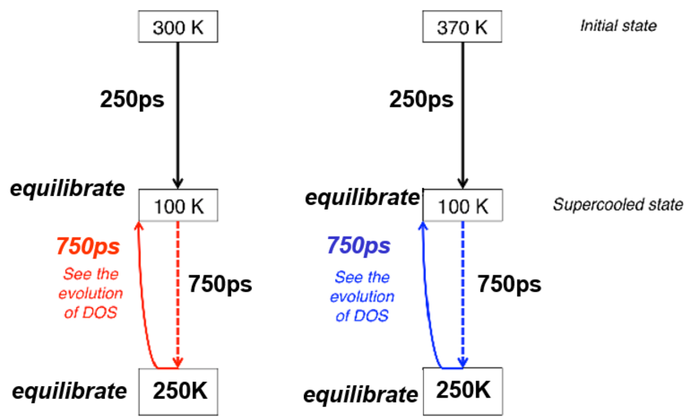

Scheme S1: Calculation details

The result is summarized in Figure S9, which shows an interesting trend in the low-frequency region at 0 cm^{-1} (the region in the dashed circle in Figure S9). The fast decreasing pattern from 370K case supports our hypothesis.

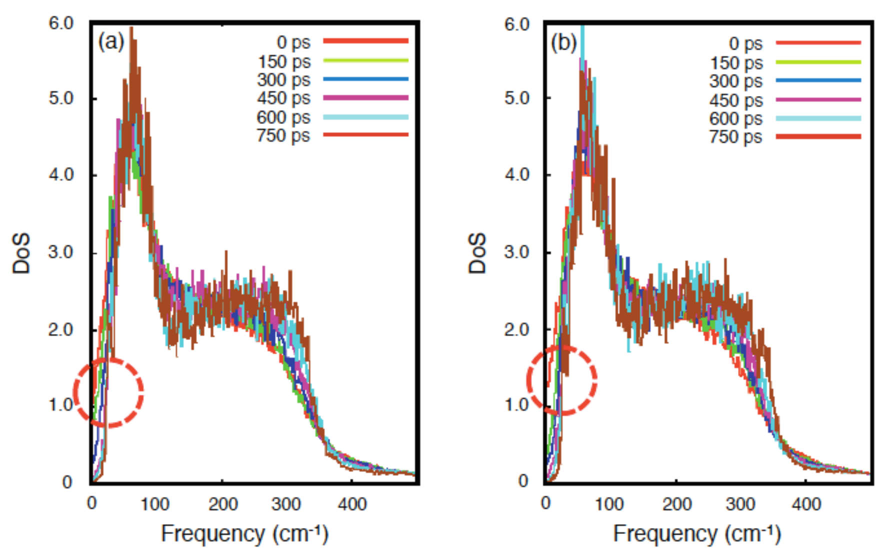

Figure S9: Changes in translational libration DOS after annealing the 100K quenched system at 250K and re-quenching over times ranging from 150 to 750 ps
(a) Initial temperature from 300K (b) Initial temperature from 370K

G. O-O radial distribution function (RDF) analysis

As alternative analyses of the nature of supercooled water from different quenching conditions, we examined the O–O radial distribution functions to figure out how higher population of water hexagon nuclei enhances freezing in an atomistic view. Here we compared the radial distribution function obtained from supercooled water using 300 water molecules with the experimental structure of ice Ih with 288 water molecules.[5] Figure S10-(a) shows that ice Ih has sharp peaks at O–O distances of

- 2.8 Å, nearest neighbor H_2O's; which is the standard O–O distances in hydrogen bonding,
- 4.5 Å, second nearest neighbor waters in the water hexagon. For tetragedral H_2O, the ratio of 2^{nd} to 1^{st} nearest neighbor distances is 4/sqrt(6)=1.632, compared to 4.5/2.8=1.64 and
- 5.3 Å, which corresponds to third nearest neighbors going across the hexagon.[27]

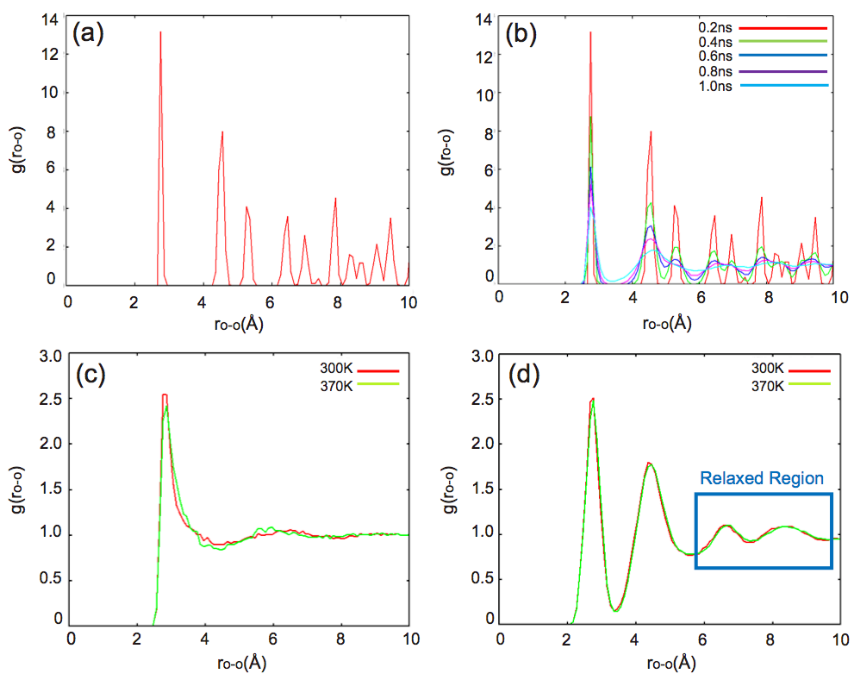

Figure S10: O–O radial distribution function (RDF) (a) Ice Ih at 100K (b) RDF from MD simulations with the F3C water model, evoluting from ice Ih at 100K as the temperature is raised to 1ns and allowed to melt over 0.2ns, 0.4ns, 0.6ns, 0.8ns, 1.0ns (c) Water at 300K and 370K (d) Supercooled water at 100K quenched from 300K and from 370K over 50 ps.

Figure S10-(b) shows the evolution of the ice O–O distances as the ice is melted at 300K. This is compared in Figure S10-(c) to the O–O for water at 300K and 370K. Finally Figure S10-(d) shows the radial distributional function of water rapidly cooled to 100K from 370 or 300K.[6] The major differences between pure ice and supercooled water are in long-range region from 6 to

10 Å. (See Figure S10-(d)) When ice melts to water, the peaks become broader and some coalesce.

To compare the supercooled water with ice we use the Continuous Wavelet Transform (CWT) so that the local spectral components at distinct distances are considered fully rather than the whole spectral content given as the Fourier transform.[7] Here, the transformed signal is a function of two variables, τ (translation) and s (scale). $\Psi(t)$ is the transforming function, called the mother wavelet. The CWT of a data set $x(t)$ is a convolution of the data which is followed as

$$\mathrm{CWT}_x^{\psi}(\tau, s) = \frac{1}{\sqrt{s}} \int x(t)\psi^*(\frac{t-\tau}{s})dt \tag{1}$$

The continuous wavelet transform was conducted for the radial distribution function of pure ice Ih and water supercooled from 300K and 370K, see Figure S11-(b), (d). The general tendencies of the water radial distribution function are observed as localized wavelets with high frequency, leading to a short wavelength indicating sharp peaks in specific ranges. This pattern is scattered for large O–O distances, which is related to the long-range relaxation. We see that supercooled water has a higher population with short-range relaxation than for pure ice Ih. In order to compare these systems we calculate the semblance of each CWT, since the differences between Fourier transformed signals are directly calculated by following formula.[8]

$$S = \cos\theta(f) = \frac{R_1(f)R_2(f) + I_1(f)I_2(f)}{\sqrt{{R_1}^2(f) + {I_1}^2(f)} \times \sqrt{{R_2}^2(f) + {I_2}^2(f)}} \tag{2}$$

The semblance of two CWT was calculated by the correlation of two CWT spectrums for each point. In Figure S11-(e), the dark brown part indicates high semblance while the blue region indicates a hole with low semblance. Since these holes are more often at long distances, the relaxation can be interpreted as long-range correlation.

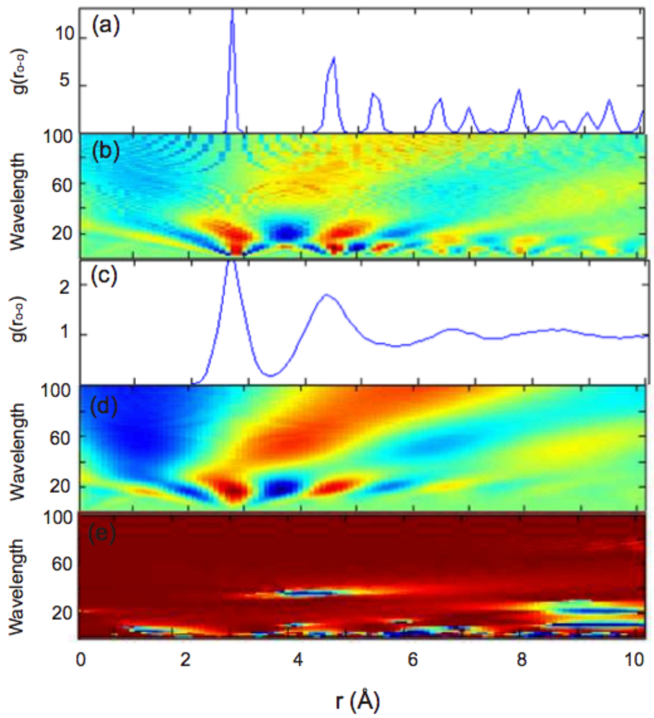

Figure S11: CWT analysis and Semblance plot of the radial distribution function (RDF)[7,8]

(a) RDF of pure ice Ih

(b) CWT of (a). Here blue → large positive amplitude and red → large negative amplitude

(c) RDF of supercooled water from 370K

(d) CWT of (c). Here blue → large positive amplitude and red → large negative amplitude

(e) Semblance analysis of (b) and (d). Here brown → high semblance and blue → low semblance

These results suggest that the water hexamer and fused water decamer serve as nuclei for ice formation while cooling. We compared the radial distributional function of supercooled water obtained from quenching water from the initial temperature of 370K while freezing the hexamer structure. To determine the similarity of the radial distributional function of supercooled water with pure ice Ih model, we compare the correlation coefficient. The overall correlation increased from 0.4114 to 0.5665. However, in the short-range region (2-3 Å), the correlation coefficient increased from 0.7930 to 0.8259, indicating that the water hexamer/fused decagon may play a significant role in enhancing crystallization in the short-range region.

H. Radial distribution function analyses upon structural resemblance of water with oxygen

The structure of the ice is governed by the structure of the oxygen, see Figure S12. Therefore, calculating the radial distribution function of oxygen-oxygen indicates the structural resemblance as an ice. The verification of the obtained structure was conducted as twofold comparison of RDF between supercooled water with pure ice and its relaxed state. To calculate the radial distribution function of the ice, we selected the ice Ih model with 288 water molecules.

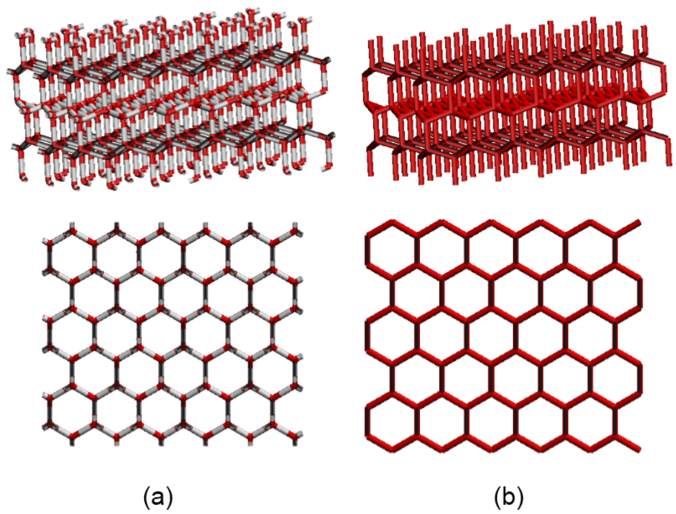

Figure S12: Ice Ih with 288 H_2O molecules with retaining its hexagonal structure
(a) Total representation (b) Oxygen representation

To compare it with supercooled water accurately, we compared it with general ice Ih model and relaxed ice model. At first, we got a NPT dynamics with normal pressure condition. The first RDF was calculated at the very initial state and relaxed state was calculated by taking the last structure of the calculation. The detailed comparison scheme is described in the Scheme S2.

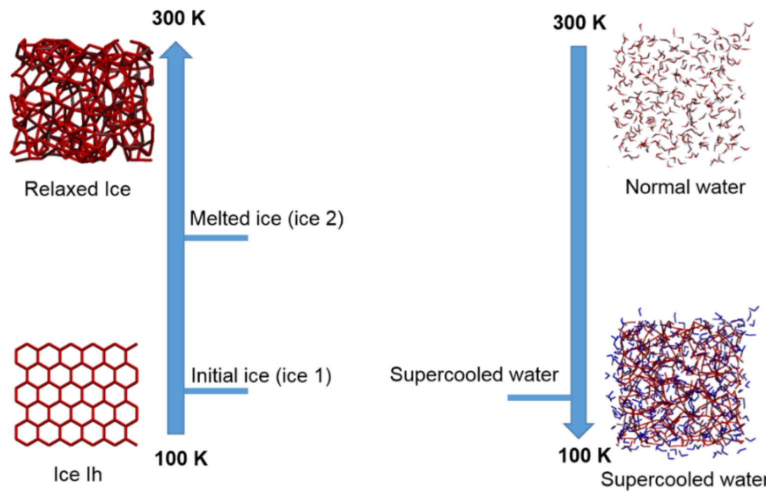

Scheme S2: Comparison of initial ice with supercooled water

Also, Continuous Wavelet Analysis (CWT) and semblance analysis were conducted for this two state of the ice Ih. The comparison at the initial state of the ice was described on the paper, however, in this supplementary discussion, we want to denote the comparison with relaxed state of the ice Ih. The differences is depicted as less holes in the semblance plot which indicates that the ordering of relaxed water has more in the short-range and less in the long-range region.

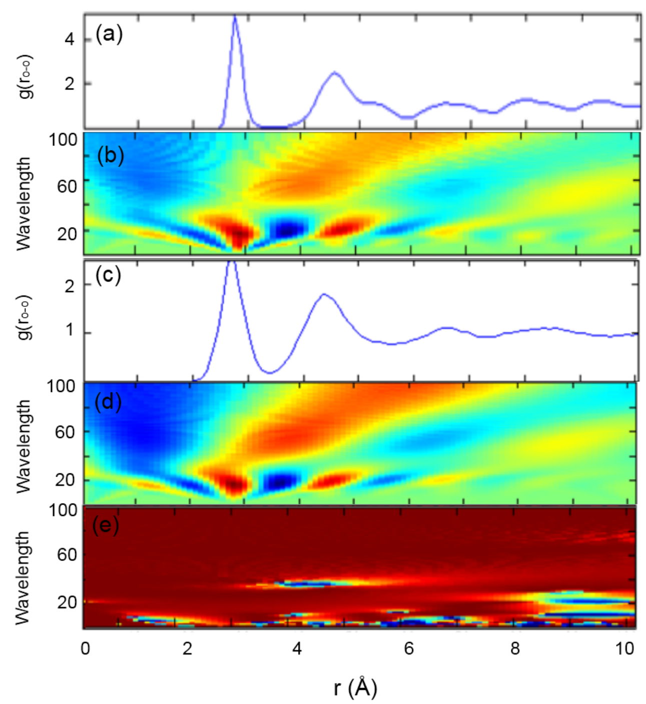

Figure S13: CWT analysis and Semblance plot of radial distribution function
(a) RDF of relaxed ice Ih (b) CWT of (a) (c) RDF of supercooled water (d) CWT of (c)
(e) Semblance analysis of (b) and (d)

This short-range behavior of the supercooled water can be understood as the initial nucleation procedure of water. We firstly figured out that the frozen hexamer can lead to more crystallization and increased intensity in the short region. Also, in the ice Ih model, distances between oxygen atoms are distributed from short-range to long-range with its intensity. We divided these distances into in-plane and out-plane distances and calculated the proportion of each distance, see Figure S14. It denotes that in the short-range region, in-plane distances between oxygen atoms dominates rather than out-plane distances. It can give another explanation to the crystallization process, which initiates with small local planar clusters.

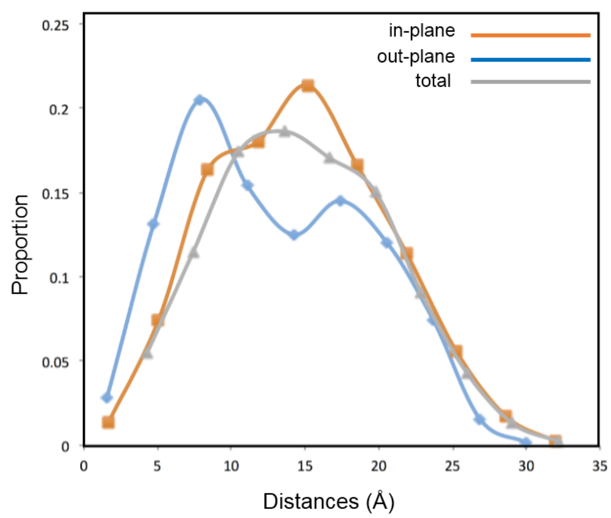

Figure S14: Distance distribution between oxygen atoms

References

1. Liu, H.; Wang, Y.; Bowman, J. M. Vibrational Analysis of an Ice Ih Model from 0 to 4000 cm–1 Using the Ab Initio WHBB Potential Energy Surface. *The Journal of Physical Chemistry B* **2013**, *117*, 10046–10052.

2. Bertie, J.; Whalley, E. Optical Spectra of Orientationally Disordered Crystals. II. In- frared Spectrum of Ice Ih and Ice Ic from 360 to 50 cm. *The Journal of Chemical Physics* **1967**, *46*, 1271.

3. Lobban, C.; Finney, J.; Kuhs, W. The structure of a new phase of ice. *Nature* **1998**, *391*, 268–270.

4. Sanz, E.; Vega, C.; Abascal, J.; MacDowell, L. Phase diagram of water from computer simulation. *Physical review letters* **2004**, *92*, 255701.

5. Jacobson, L. C.; Molinero, V. A Methane- Water Model for Coarse-Grained Simulations of Solutions and Clathrate Hydrates. *The Journal of Physical Chemistry B* **2010**, *114*, 7302–7311.

6. Lee, H.-J.; Cagin, T.; Johnson, W. L.; Goddard III, W. A. Criteria for formation of metallic glasses: The role of atomic size ratio. *The Journal of chemical physics* **2003**, *119*, 9858.

7. Mallat, S. *A wavelet tour of signal processing*; Access Online via Elsevier, 1999.

8. Cooper, G.; Cowan, D. Comparing time series using wavelet-based semblance analysis. *Computers & Geosciences* **2008**, *34*, 95–102.